COMPARATIVE ANALYSIS OF THE ESA AND NASA INTERPLANETARY METEOROID ENVIRONMENT MODELS

Eberhard Grün[1,2], Ralf Srama[3], Mihaly Horanyi[2], Harald Krüger[4], Rachel Soja[3], Veerle Sterken[1,3], Zoltan Sternovsky[2], Peter Strub[4]

[1] MPI for Nuclear Physics, Saupfercheckweg 1, 69117 Heidelberg, Germany, Email:eberhard.gruen@mpi-hd.mpg.de
[2] LASP, University of Colorado, Boulder, USA
[3] IRS, University Stuttgart, Stuttgart, Germany
[4] MPI for Solar System Research, Lindau-Katlenburg, Germany

ABSTRACT

Meteoroid environment models are used to assess the hazard arising from meteoroid impacts onto space structures. We have analyzed the current meteoroid models of ESA (**IMEM**) and of NASA (**MEM**). These models are based on different sets of measurements. MEM is based on radar meteor observations, lunar impact cratering rate, and on zodiacal light observations while IMEM is based on orbital element distributions of comets and asteroids, the lunar impact cratering rate, thermal radiation observations, and on in situ dust measurements. Both models describe the cratering flux at 1AU quite well; however, the flux of mm-sized meteoroids differs by a factor two due to the different assumed relative speeds. At other heliocentric distances from Mercury to Mars the predicted fluxes differ by up to 2 orders of magnitude between the two models. The current knowledge of the interplanetary meteoroid environment as exemplified by these meteoroid models is insufficient to provide reliable assessment of the risk of meteoroid impacts for human travel in interplanetary space.

1 INTRODUCTION

The meteoroid complex is one of the most uncertain space environments. In near-Earth space, knowledge of the impact hazard has to be supported by online military-grade optical and radar observations in order to protect the International Space Station against potentially lethal projectiles. Such methods are not available for interplanetary space travel, hence, meteoroid engineering models are needed to keep manned missions out of harm’s way. While for unmanned spacecraft (1 to 10 m^2 surface area) the meteoroid hazard is generally small and can easily mitigated, larger manned structures (100 to 1000 m^2) are more vulnerable.

A wide range of observations exists for different aspects of the interplanetary meteoroid cloud, most of which refer to the environment near 1 AU. We only have information on the meteoroid environment far from the Earth from remote sensing observations both at visible and infrared wavelengths and from in situ measurements by spacecraft.

For a modern interplanetary meteoroid model for the assessment of the meteoroid hazard it is essential to provide not only the spatial density of meteoroids as function of their size, but also their speed and directional distributions in space. However, dynamical information on the meteoroids is very limited: with the exception of in situ detectors only the meteor phenomenon in the Earth's atmosphere provides speed and directional flux information of the meteoroids causing it. In addition, recent studies of the generation and dynamical evolution of meteoroids from their parent objects (comets and asteroids) provide indirect access to the dynamical state of meteoroids in interplanetary space [1, 2, 3].

Currently, only two meteoroid environment models exist that include halfway realistic dynamical information on the meteoroid flux in interplanetary space: NASA's Meteoroid Engineering Model **MEM** and ESA's Interplanetary Micrometeoroid Environment Model **IMEM**. Both models (software and relevant documentation) are readily available from the respective space agencies. No restrictions are placed on their use.

2 INTERPLANETARY DUST ENVIRONMENT MODELS

The earliest reliable NASA meteoroid environment model was derived from meteor observations from the Harvard Meteor Radio Program (HRMP) and simple large-area dust detectors onboard the Explorer and Pegasus satellites [4]. The latter provided fluxes and estimated impact speeds for up to mm-sized meteoroids. With the availability of lunar surface samples returned by Apollo, it became possible to extract the meteoroid size distribution from the lunar micro-crater distribution for sub-micron to about mm size particles. A constant speed of 20 km/s was used for the conversion of crater sizes to projectile sizes [5], which was compatible with measured meteor speeds at that time. While this model and its followers [6,7] represented the input data satisfactorily, it had no basis for any extrapolation to other regions in space or to other masses beyond those

Proc. ‘6th European Conference on Space Debris’
Darmstadt, Germany, 22–25 April 2013 (ESA SP-723, August 2013)

of the original input data.

2.1 NASA's Meteoroid Engineering Model, MEM

MEM was developed by [8, 9] on the basis of sporadic meteor observations from the Canadian Meteor Orbit Radar (CMOR). This is combined with zodiacal light observations from Helios which provide the radial meteoroid density distribution. The mass distribution in the range from 10^{-6} to 10 g was derived from lunar crater statistics [5]. Since the model heavily uses orbital element distributions from meteor data which must intersect the Earth, it can only be used at best for predictions of fluxes, speeds, and directions from 0.2 to 2.0 AU. This includes the environments of the planets Mercury (0.4 AU) to Mars (1.5 AU). Additionally, the model applies only to an observer moving near the ecliptic plane [8].

The radiants of meteors, including radar meteors, are not uniformly distributed on the celestial sphere. Instead, they form clusters that have different relative speeds with respect to Earth. The sporadic meteoroid complex as observed from Earth is known to have four major populations distributed symmetrically about the ecliptic plane. The primary sporadic meteoroid populations, as given in the orbital survey [10], are the Helion/Anti-Helion, the North/South Apex, and the North/South Toroidal populations (Tab. 1). These three populations are associated with a cometary origin [2]. The fourth population, which is not well understood, is the asteroidal source. Meteors in this category have very low relative speeds, and are therefore not observed by CMOR but instead derived from IR observations. Observed asteroidal meteoroids are predicted to have latitudes close to the ecliptic poles, at about ±90º, in the apex direction.

Table 1. Major meteor populations. The speeds (as determined from optical and radar meteor observations, including CMOR data) refer to relative speeds after the effects of the Earth’s gravity and atmospheric deceleration have been removed [8].

Population	**Observed mean speed (km/s)**	**Parent objects**
Helion/Anti-Helion	34.5	Jupiter Family Comets
North/South Apex	57.2	Long-period comet
North/South Toroidal	42.0	Halley type comets
Asteroidal population	13.0	Asteroids

By definition, the orbits of meteoroids that generate meteors in the Earth's atmosphere must cross the Earth's orbit: that is, they must have a perihelion distance ≤1 AU and an aphelion ≥1 AU. Most asteroids are 'Main Belt Asteroids', which populate the asteroid belt between 2 and 3.5 AU, and do not have orbits that intersect the orbit of the Earth. More than 100,000 such asteroids exist. Only several hundred Earth-crossing asteroids are currently known, which thus have the potential to either impact the Earth themselves, or to produce debris that can impact the Earth. Jupiter family comets are the dominant group of short period comets. They have orbital periods below 20 years, cross the orbit of Jupiter and their orbits are frequently scattered by this planet to other Jupiter-crossing orbits. Only Jupiter Family Comets with eccentricities > 0.7 cross the orbit of the Earth and thus are able to provide high-speed meteors from their ejected particles. Even higher meteor speeds can be expected from long period comets and from comets in retrograde orbits like Halley type comets.

The ionization trail observed by ground-based radars is used to derive the mass and speed of a meteoroid, For example, Jones [8] assumes a strong dependence of the ionization efficiency on the meteoroid entry speed into the Earth's atmosphere ($\sim v^4$). This dependence is then used to derive the meteoroid mass from the radar signal strength. It is concluded that CMOR data and hence the MEM [9], refers to meteoroids of masses $m \geq 10^{-6}$ g. MEM uses a mass distribution derived from lunar microcraters assuming a constant impact speed of 20 km/s [5]. Since both data sets (meteors and lunar microcraters) refer only to the meteoroid population at 1 AU, MEM is extrapolated by following the radial meteoroid density profile as derived from the Helios zodiacal brightness measurements inside 1 AU: density $n \sim r^{-1.3}$ [11].

2.2 ESA's Interplanetary Micrometeoroid Environment Model IMEM

IMEM is a dynamical evolutionary model [1]. Contrary to all earlier attempts, this model starts from the orbital elements of known sources of interplanetary dust: comets and asteroids. The model assumes that big meteoroids ($\geq 10^{-5}$ g) stay in Jupiter crossing orbits like their parent objects, while the orbits of smaller meteoroids evolve under planetary gravity and the Poynting-Robertson effect. Thermal radiation measurements by the COBE DIRBE instrument [12], in situ data from the dust instruments onboard Galileo and Ulysses [13] and lunar microcrater distributions [5] are used to calibrate the contributions from the known sources. Attempts to include meteor orbits from the Advanced Meteor Orbit Radar AMOR [14] in the model failed since the AMOR orbital distributions were incompatible with the COBE latitudinal density profile. The derivation of the meteoroid spatial distribution from the actual radar meteor measurements is quite complex and involves numerous assumptions; whereas the derivation of the infrared brightness along a line-of-sight is relatively straight-forward. Therefore, Dikarev et al. [1] decided not to include meteor data in the IMEM model. A recent similar analysis [3] confirms that comets are currently the main contributor to interplanetary dust at 1 AU and suggested that the radar meteor systems underestimate the contributions from slow meteoroids.

IMEM makes use of the fact that Jupiter family comets (JFCs) are an obvious source of meteoroids in the interplanetary space. However, because of a number of loss mechanisms, such as ejection from the Solar system (mostly by Jupiter) and fading out of the comet, there are only a few hundred comets active at the present time. The typical active lifetime of a comet in the inner planetary system is estimated to be a few thousand years, while the residence time of 0.1 mm and bigger grains (which carry most of the mass) in the zodiacal cloud is of the order of ten to hundred thousand years. This means that many generations of JFCs must have contributed to the present zodiacal cloud. Therefore, instead of using the actual orbit distributions of presently known JFCs, Dikarev et al. [1] simulated the motion of test particles emitted by every possible source in the region of encounters with Jupiter. Assuming ergodicity in the region of close encounters with the planet, Dikarev and Grün [15] obtain simple analytical expressions for the orbital distributions of test particles that closely resemble the results of their numerical simulations.

Contrary to earlier models [6, 7] which used separated orbital distribution functions for the orbital elements semi-major axis, a, eccentricity, e, and inclination, i, assuming $f(a,e,i) \sim f(a)\times f(e)\times f(i)$. Instead, MEM uses the approximation $f(a,e,i) \sim f(a,e)\times f(i)$ and IMEM uses the complete distribution function $f(a,e,i)$ itself. In addition, IMEM separates orbital distributions according to the mass range: for small particles with $m < 10^{-6}$ g both the original orbit distribution in the Jupiter scattering zone and the orbital distribution that results from the Poynting-Robertson effect are considered; for big particles $m \geq 10^{-5}$ g only the original orbit distribution in the source region is considered. This is motivated by the fact that the lifetimes of big particles are determined by collisional shattering rather than by Poynting-Robertson transport [5].

IMEM lumps 79 individual classes of meteoroids of different sizes and dynamical parameters together into five major populations:

1. Asteroid Collisions ($m \geq 10^{-5}$ g),
2. Asteroid Poynting-Robertson ($m < 10^{-5}$ g),
3. Comet Collisions ($m \geq 10^{-5}$ g),
4. Comet Poynting-Robertson ($m < 10^{-5}$ g), and
5. Interstellar Dust (10^{-15} to 10^{-9} g).

These theoretical distributions are then summed together with weights assigned to fit the following observations:

– infrared observations by the COBE near-Earth observatory [9],
– in situ impact counts by the Galileo and Ulysses dust detectors [10], and
– the lunar crater size distribution. The cumulative mass distribution of meteoroids at 1 AU [5] is converted back into the raw crater size distribution assuming a fixed 20 km/s impact speed. Then the model is fitted to the raw distributions, taking the model speeds of meteoroids into account when predicting meteoroid masses.

IMEM states an applicable distance range form 0.1 to 5.0 AU - from Mercury to Jupiter - and an applicable mass range form 10^{-18} to 1 g. IMEM has no latitudinal restrictions.

3 RESULTS

We compare the IMEM and MEM model by analyzing the fluxes for both models for circular orbits in the ecliptic plane. A trajectory file is prepared with the state vectors and, in case of IMEM, with the additional pointing directions for which the fluxes are calculated. For circular orbits in the ecliptic at distances from 0.1 AU to 10 AU we calculate meteoroid fluxes and speeds in the applicable mass range and for six orthogonal directions (Ram, Wake, Port, Starboard, North, and South directions). We used only the interplanetary meteoroid environment for Sun orbiting spacecraft, IP-MEM, from MEM Release 1.0c (contact: Heather McNamara, NASA MSFC). We used IMEM1.1 GUI, Version 0.8.5 and IMEM2 engine version 0.7.7 build 467 (2011-05-09, contact: Alexey Mints, Hamburg Observatory). The resulting ASCII files generated by MEM and IMEM were analyzed.

3.1 IMEM

All IMEM populations have constant fluxes along circular orbits; only the interstellar population displays some variation. The constant fluxes and impact speeds of interplanetary meteoroids are an effect of the axial symmetry assumed in IMEM and MEM.

The different orbital distributions assumed for big ($m \geq 10^{-5}$ g) and small ($m < 10^{-5}$ g) meteoroids cause different fluxes onto the six faces of a cube spacecraft. While at 1 AU the fluxes from most directions are within 30% of each other, the Wake flux shows significant variations: for small particles it is a factor ~3 smaller than the fluxes observed from the other directions (the spacecraft overtakes most small meteoroids), whereas for big particles it is higher than all other fluxes (most meteoroids have higher azimuthal speeds than the spacecraft). A similar behavior is seen for orbits inside 1 AU. At Jupiter's distance (5.2 AU) - that is, in the source region of dust from JFCs - the Ram fluxes of both big and small meteoroids are a factor ~10 higher than fluxes onto the other spacecraft faces, while the Wake fluxes are comparable to other fluxes.

The cumulative flux (i.e. the flux of meteoroids with masses ≥ the given mass, m) onto a flat plate facing the Ram direction is displayed in Fig. 1 for circular orbit at 1 AU heliocentric distance. For comparison the flux derived from lunar microcraters [5] is roughly represented by the IMEM flux for m < 10^{-5} g and the MEM flux for m ≥ 10^{-5} g.

At 1 AU the IMEM flux of big particles (m ≥ 10^{-5} g) is more than an order of magnitude below the Grün et al., [5] flux and the MEM flux because IMEM assumes a much higher impact speed than for smaller particles (Fig. 2). While the small particle flux decreases with heliocentric distance, the flux of big particles increases with distance up to Jupiter's orbit such that the big particle IMEM flux is even higher than the flux at 1 AU [5].

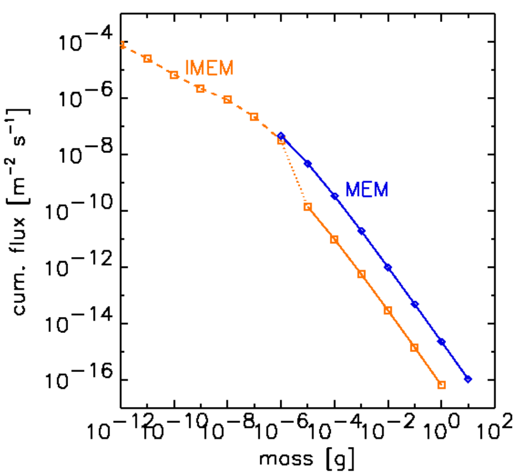

Figure 1. Cumulative flux onto Ram face at 1 AU for both IMEM (red) and MEM (blue).

The dichotomy of big and small particle fluxes originates from the difference in the assumed impact speeds for the various meteoroid populations: the speed of the dominant population of big particles (Comet Collisions population: 40 km/s) is about a factor 2.7 times higher than that of small particles (Comet Poynting-Robertson population: 15 km/s). Craters from projectiles at the higher speed are as big as craters from ~7.5 times more massive projectiles with the lower impact speed. This is because the crater size roughly scales with the energy ($m \times v^2$) of the projectile.

The radial flux (top) and average speed (bottom) onto the Ram face are shown in Fig. 2 for two limiting masses 10^{-6} and 10^{-5} g. The cumulative fluxes strongly depend on the meteoroid mass, whereas the speed distribution has only two modes: one for big and one for small particles (IMEM). While interstellar and comet-derived particles can be found everywhere in the inner planetary system, asteroidal meteoroids are generated only from 0.7 to 4 AU. The peak generation of meteoroids from comets occurs at Jupiter's distance where the flux of big particles (m ≥ 10^{-5} g) is at its maximum. Small particles evolve under the Poynting-Robertson effect and their density inside the source region is n ~ r^{-1} [15]. Between Venus and Mars we find a distribution for the radial slope of the flux of small particles with m < 10^{-5}g of ~ $r^{-1.27}$, whereas the impact speed is flat and has a minimum in this region. For bigger particles (m ≥ 10^{-5}g) the flux does not increase much inside 1 AU but instead increases by almost two orders of magnitude between the Earth's and Jupiter's orbits. The radial slope of the impact speed varies as ~ $r^{-0.67}$, which increases stronger than the circular Kepler speed $r^{-0.5}$.

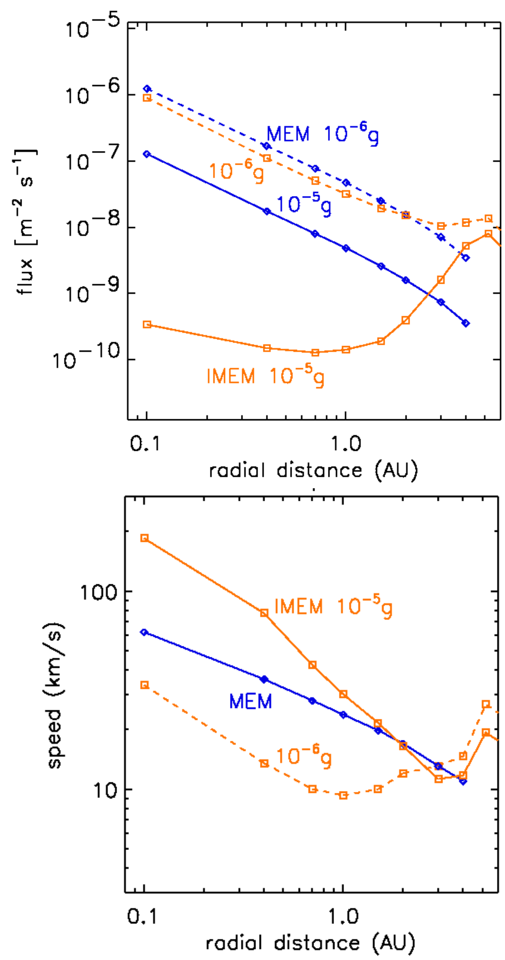

Figure 2 Radial Ram flux (top) and speed distributions (bottom) for 10^{-6} g and 10^{-5} g particles for both IMEM (red) and MEM (blue).

The directionality of the IMEM meteoroid fluxes (without the Interstellar Dust population) onto a sphere at 1 AU in the ecliptic is shown in Fig. 3. The sky maps of small and big particles are very different because of the very different dynamics assumed for these particle types. These sky maps can be compared to those obtained from meteor observations. However, a better comparison to meteor observations is obtained from sky maps in different speed ranges. The sky maps of big particles in the 20 to 40 km/s range resembles the Helion/Anti-Helion meteor population from [8]. The sky map of small particles in the 0 to 20 km/s range resembles the North/South Toroidal meteor population. The sky map of the small Asteroid Poynting-Robertson population resembles vaguely the Asteroidal meteor population of [8]. The North/South Apex population is not represented in IMEM since meteoroids originating from long-period and retrograde comets are not considered.

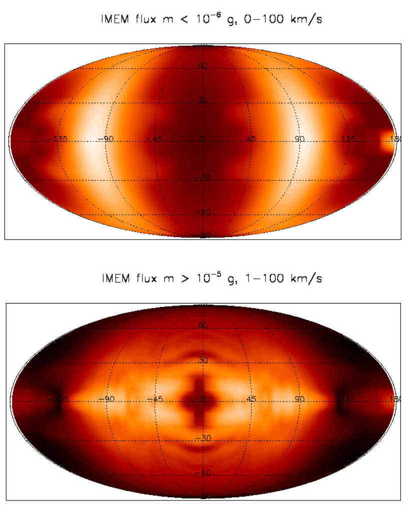

Figure 3. Sky maps of small particle flux (m < 10^{-5} g, left) and big particle flux (m ≥ 10^{-5} g, right) for all speeds. The maximum intensity (brightest colors) is normalized and the intensity scale is logarithmically compressed.

3.2 MEM

The MEM cumulative meteoroid flux along a circular orbit at 1 AU is constant like that of IMEM. This is also true for fluxes along circular orbits at different distances from the Sun. The mass distribution of the meteoroid flux onto the RAM face at 1 AU distance from the Sun is shown in Fig. 1. The fluxes at 1 AU onto the Ram, North, and South faces are within 5% of the flux derived from lunar microcraters [5], while the fluxes onto the Starboard and Port faces are about 25% higher and the flux onto the Wake face is about a factor 5 lower. The dependence of the Ram flux and impact speed on heliocentric distance for 10^{-6} g and 10^{-5} g meteoroids is shown in Fig. 2. For other limiting masses the radial slopes of flux and speed are the same: only the absolute fluxes scale with mass, as shown in Fig. 1. Between Venus and Mars we find that the radial slope of the MEM flux is ~ $r^{-1.47}$, and the radial slope of the impact speed is ~ $r^{-0.45}$. This slope is close to that of the circular Kepler speed (v ~ $r^{-0.5}$), whereas the slope of the flux distribution is compatible with meteoroids evolving under the Poynting-Robertson effect [16].

Comparison of the fluxes onto different faces of a cube indicates that the orbital elements assumed in MEM change with heliocentric distance. In particular, the Ram/Wake flux ratio indicates that the assumed semimajor axis and eccentricity distributions change significantly between 0.4 and 2 AU.

The average impact speed is independent of meteoroid mass. At 1 AU the mean speed averaged over all directions is ~ 22 km/s, which is not significantly different from the speed (20 km/s) assumed for the calibration of the lunar microcraters.

The meteoroid flux onto a sphere at 1 AU in the ecliptic obtained by MEM is shown in Fig. 4. This sky map can be compared to those showing meteor observations (Tab. 1). The peaks at ±70° longitude and 0° latitude are caused by the Helion/Anti-Helion meteor populations and the ring at ±90° longitude are the North/South Toroidal population. The weak intensities at ~0° longitude and low latitudes are the high-speed North/South Apex populations. There is no indication of the slow speed Asteroidal meteor population of [8].

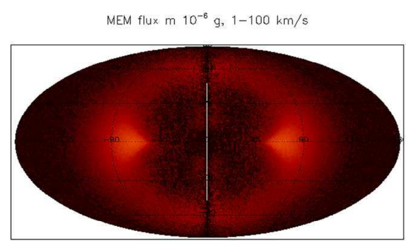

Figure 4. Sky map of the MEM particle flux for all speeds of meteoroids > 10^{-6} g projected onto a sphere at 1 AU in the ecliptic. For more information see Fig. 3.

4 DISCUSSION

A comparison of the predicted Ram fluxes and impact speeds using MEM and IMEM is presented in Tab. 2. The fluxes of small meteoroids (m ≥ 10^{-6} g) agree generally within ~30% in the distance range from 0.1 to 2 AU. The biggest difference (50%) occurs in the Ram flux at 1 AU. For the big particle fluxes (m ≥ 10^{-3} g), differences of two orders of magnitude are found in the distance range from 0.1 to 2 AU, with a factor 30 difference in the Ram flux at 1 AU. We find factor of 3 differences in the impact speeds predicted by the two models.

Table 2: Comparison of IMEM and MEM fluxes [m^{-2} yr^{-1}] in Ram direction and averaged over all directions (upper portion) and the flux averaged impact speeds [$km\ s^{-1}$] in Ram direction and averaged over all directions (lower portion). In bold face are fluxes that can be compared with an earlier analysis [17].

		m > 10^{-6} g				**m > 10^{-3} g**			
		Ram Flux		**Ave. Flux**		**Ram Flux**		**Ave. Flux**	
R (AU)	**Planet**	**IMEM**	**MEM**	**IMEM**	**MEM**	**IMEM**	**MEM**	**IMEM**	**MEM**
0.10		2.8E+1	3.9E+1	3.2E+1	3.1E+1	4.4E-5	1.6E-2	4.5E-5	1.3E-2
0.40	**Mercury**	3.5E+0	5.3E+0	**5.1E+0**	**6.1E+0**	1.9E-5	2.2E-3	**5.4E-5**	**2.5E-3**
0.70	**Venus**	1.6E+0	2.4E+0	**2.4E+0**	**2.6E+0**	1.6E-5	1.0E-3	**7.2E-5**	**1.1E-3**
1.00	**Earth**	1.0E+0	1.5E+0	**1.4E+0**	**1.3E+0**	1.8E-5	6.2E-4	**1.4E-4**	**5.6E-4**
1.50	**Mars**	6.1E-1	7.9E-1	**6.8E-1**	**5.6E-1**	2.4E-5	3.3E-4	**3.2E-4**	**2.3E-4**
2.00		4.7E-1	4.9E-1	4.1E-1	2.9E-1	5.1E-5	2.0E-4	3.9E-4	1.2E-4
		Ram speed		**Ave. speed**		**Ram speed**		**Ave. speed**	
0.10		83.89	62.10	46.33	54.95	184.68	62.10	98.00	54.95
0.40	**Mercury**	34.80	35.90	**25.43**	**31.97**	77.34	35.90	**43.58**	**31.97**
0.70	**Venus**	26.13	28.00	**16.46**	**25.42**	42.25	28.00	**24.08**	**25.42**
1.00	**Earth**	19.71	23.80	**12.71**	**21.68**	30.12	23.80	**17.49**	**21.68**
1.50	**Mars**	15.78	19.80	**9.98**	**16.93**	21.57	19.80	**12.55**	**16.93**
2.00		14.27	17.00	7.72	13.47	16.51	17.00	7.94	13.47

In 2009, the Inter-Agency Space Debris Coordination Committee conducted a comparison of meteoroid models [17]. The current versions of the IMEM and MEM (only for interplanetary meteoroids) are included in this comparison for $m \geq 10^{-6}$ and $m \geq 10^{-3}$ g particles at the planets Mercury, Venus, Earth, and Mars ([17], Tables 5 to 8). Their averaged fluxes at the orbits of each of these planets are the same as the values we calculate (Tab. 2) to within ~5%. The averaged impact speeds, however, agree within 5% only at the distance of the Earth; at the distance of the other planets the disagreement reaches ~50% (IMEM) and ~20% (MEM). One explanation could be that our averaging method is different to that used in the 2009 comparison.

Both interplanetary meteoroid models of ESA and NASA give divergent values for fluxes and speeds. The most significant problems with both meteoroid models are demonstrated in Fig. 2 in which we compare the radial flux and impact speed profiles at the neighbouring limiting masses 10^{-6} g and 10^{-5} g. A major problem of the IMEM is the dichotomy of fluxes and speeds between small and big meteoroids. A further problem is that the orbital distributions of the big particle populations reflect only the theoretical source distributions of meteoroids and do not include their orbital evolution except for the scattering by Jupiter. In addition, only the IMEM includes the in situ data that provide limited dynamical information. Although the sky maps of the IMEM flux resemble some aspects of the meteor sky maps, the inclusion of more dynamical information from both in situ and meteor data could improve the model significantly even at 1 AU. The cumulative fluxes from both models are similar at 10^{-6} g, where the Poynting-Robertson dominates the fate of meteoroids, however, at bigger masses where planetary scattering and collisional shattering dominates the differences are more than an order of magnitude. IMEM, at least, captures some aspect of these different dynamics and hence is probably closer to a realistic description of the big meteoroid flux than MEM.

While the MEM may provide the best meteoroid fluxes and impact speeds at the Earth's orbit, it is unreliable further away from 1 AU. A strength of the MEM is the inclusion of CMOR meteor data to provide speeds at 1 AU. However, its extrapolation to other distance is a major weakness: the underlying Poynting-Robertson orbital evolution is not applicable to the meteoroid size range it is applied to. Another major weakness of MEM is that it does not include knowledge of the meteoroid complex from remote-sensing observations (such as zodiacal light and infrared emission data).

5 SUMMARY AND CONCLUSIONS

The meteoroid complex is one of the least-understood space environments. NASA's Meteoroid Engineering Model (MEM) is based on orbital element distributions derived from sporadic meteor observations and the lunar crater size distribution. The radial distribution is derived from zodiacal light observations and the model is applicable to missions from 0.2 to 2.0 AU. MEM has the following caveats:

- Zodiacal light brightness corresponds mostly to particles of ~3×10^{-7} g, which is where the cross-sectional distribution peaks. This mass is below the mass represented by CMOR observations ($m > 10^{-6}$ g).
- The mass distribution is expected to be significantly different at other heliocentric distances than at 1 AU [18].
- MEM reproduces satisfactorily the speed-separated populations of CMOR meteor radar data, but their

relative contributions and the importance of slow (< 20 km/s) meteoroids remain obscure.
– There is no consideration of thermal IR observations of Zodiacal Cloud.

ESA's Interplanetary Meteoroid Environment Model (IMEM) is based on orbital element distributions of meteoroids derived from Jupiter family comets and asteroids. The densities and fluxes of IMEM are adjusted to thermal radiation data from COBE DIRBE and to in situ dust measurements by the Galileo and Ulysses dust instruments. IMEM is applicable from 0.1 to 5 AU. IMEM has the following caveats:

– Due to the different treatment of orbital distributions there is a major discrepancy between fluxes of $m \geq 10^{-5}$ g and $m < 10^{-5}$ g meteoroids.
– Only JFCs are included as cometary source objects. Other sources, such as Halley type comets, long-period comets, and Kuiper belt objects are not included.
– There is no consideration of meteor observations.

Both models ignore the temporal variability of the meteoroid flux and assume rotational symmetry about ecliptic pole. However, even the sporadic meteor flux displays significant short-term variations of about a factor two variations during the course of a year. None of the models consider the collisional balance in the meteoroid complex, which provides both a significant loss process and a major source process for fragments. Therefore, we conclude that:

– the MEM and IMEM models are in serious disagreement,
– neither of the models includes all the available data, and
– neither of the models uses all relevant physics.

Our conclusion is that using the current models for impact hazard estimates for human space flight leads to unacceptable risk for the safety of the crew and missions in interplanetary space or requires excessive shielding for impact protection.

6 UNDERSTANDING THE INTERPLANETARY METEOROID ENVIRONMENT

The following steps are necessary in order to arrive at a reliable evolutionary meteoroid environment model representing all available observations:

– Determine the input to the meteoroid cloud from Jupiter Family Comets, Encke and Halley Type Comets, and active asteroids.
– Calculate the orbital evolution of these meteoroids.
– Characterize the collisional balance everywhere in the planetary system taking into account the material properties of the meteoroids.
– Improve the interpretation of meteor observations.
– Calibrate the model with all currently available data (meteor observations, in situ measurements, impact crater counts, thermal emission observations).

The first two steps are in progress in ESA's IMEX project, of which this analysis is part. The first results show that meteoroid streams in space that have been observed as comet trails pose a significant risk to future manned missions to Mars (Fig. 5).

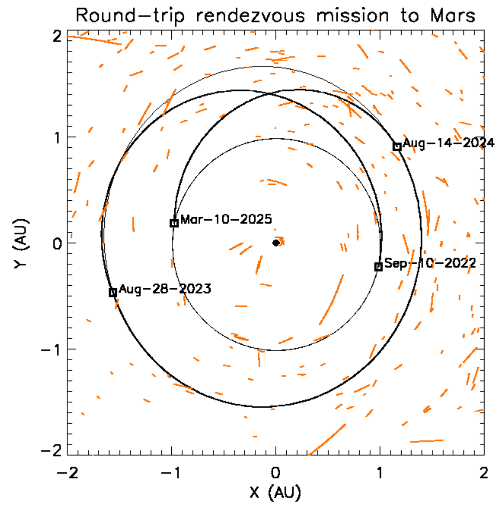

Figure 5. All of the trajectories shown on NASA's mission design center website [19] will pass through one or more potentially hazardous dust streams released from a short-period comet. The thickness of the streams is at least 10^6 km which is expected for 10^{-6} kg cometary debris particles. Having survived the trip to Mars, the astronauts may witness some spectacular meteor storm displays in the Martian atmosphere.

A strong initiative will be required from space agencies to make progress in understanding the meteoroid environment in order to support human interplanetary space travel. In addition to the improved modeling described above, major laboratory investigations are necessary to provide new collisional fragmentation data and to calibrate the meteor observations. Finally, better meteoroid data are needed between 0.7 and 1.5 AU from measurements by:

– multiple 0.1 to 1 m^2 Dust Telescopes to establish the orbital and compositional relationships between micrometeoroids and their source bodies: comets and asteroids,
– a cryogenically cooled mid-IR survey telescope to establish the extent and structure of the meteoroid cloud, and
– a thousand-square-meter Pegasus-type mission [4] dedicated to meteoroid detection to verify our models to estimate meteoroid hazard.

And finally, it is suggested that arrays of meteor radar systems are deployed on Earth and, eventually Mars. A meteor radar system built robotically during precursor landing missions would greatly enhance the crew and mission safety to Mars.

7 ACKNOWLEDGEMENTS

We acknowledge important help in understanding and running models MEM from Heather McNamara, NASA MSFC and IMEM from Alexey Mints, Hamburg Observatory. The IMEX project is supported by ESA Contract No. 4000106316/12/NL/AF

8 REFERENCES

1. Dikarev V, Grün E, Baggaley J, Galligan D, Landgraf M, Jehn R, The New ESA Meteoroid Model. Advances in Space Research 35:1282-1289, 2005

2. Wiegert P., Vaubaillon J., Campbell-Brown, M., A dynamical model of the sporadic meteoroid complex, Icarus 201 295-310(2009)

3. Nesvorny, D., Jenniskens, P., Levison, H. F., Bottke, W. F., Vokrouhlicky, D., Gounelle, M., Cometary Origin of the Zodiacal Cloud and Carbonaceous Micrometeorites. Implications for Hot Debris Disks, The Astrophysical Journal, 713, 816-836, 2010

4. Naumann, R. J. (1966). The near Earth Meteoroid Environment. NASA TND 3717.

5. Grün, E., Zook, H. A., Fechtig, H., and Giese, R. H. Collisional Balance of the Meteoritic Complex. Icarus, Volume 62, Issue 2, 244-272, 1985.

6. Divine, N. Five Populations of Interplanetary Meteoroids. Journal of Geophysical Research, Volume 98, Issue E9, 17029-17048, 1993.

7. Staubach P, Grün E, Jehn R (1997) The Meteoroid Environment near Earth. Advances in Space Research 19:301-308

8. Jones, J., Meteoroid Engineering Model - Final Report, Space Environments and Effects Program SEE/CR-2004-400, NASA Marshall Space Flight Center, 2004

9. McNamara, H., Jones, J., Kauffman, B., Suggs, R., Cooke, W., Smith, S. Meteoroid Engineering Model (MEM): A Meteoroid Model for the Inner Solar System. Earth, Moon, and Planets, Volume 95, Issue 1-4, 123-139, 2004.

10. Jones, J. and Brown, P. Sporadic Meteor Radiant Distributions: Orbital Survey Results. Monthly Notices of the Royal Astronomical Society, Volume 265, 524-532, 1993.

11. Leinert, C., Rösser, S. and Buitrago, J. 1983, How to maintain the spatial distribution of interplanetary dust, Astron. Astrophys. 118, 345-357.

12. Kelsall, T., Weiland, J.L., Franz, B.A., and 9 more authors, The COBE diffuse infrared background experiment search for the cosmic infrared background. II. Model of the interplanetary dust cloud. Astrophys. J. 508, 44-73, 1998.

13. Grün, E., Staubach, P., Baguhl, M., and 17 more authors, South-North and Radial Traverses through the Interplanetary Dust Cloud, Icarus, 129, 270-288, 1997

14. Galligan, D.P., Baggaley, W.J. The orbital distribution of radar detected meteoroids of the Solar system dust cloud. Mon. Not. R. Astron. Soc. 353 (September), 422-446, 2004.

15. Dikarev, V., Grün, E. The orbital distributions of particles resulting from multiple close encounters with planet in a steady-state approximation, in: Byrd, G.G., Kholshevnikov, K.V., Myllri, A.A., Nikiforov, I.I., Orlov, V.V. (Eds.), Order and Chaos in Stellar and Planetary Systems, ASP Conference Proceedings, vol. 316. Astronomical Society of the Pacific, San Francisco, 2004.

16. Briggs, R. E., Steady-State Space Distribution of Meteoric Particles under the Operation of the Poynting-Robertson Effect, The Astronomical Journal, 67, 268-, 1962

17. Drolshagen, G, Comparison of Meteoroid Models, Inter-Agency Space Debris Coordination Committee Action Item 24.1, 2009

18. Ishimoto, H., Modeling the number density distribution of interplanetary dust on the ecliptic plane within 5 AU of the Sun, Astron. Astrophys., 362, 1158-1173, 2000.

19. http://trajbrowser.arc.nasa.gov/example_queries.php